Self-Encoded Marker Design for Adaptive Optical Real-Time Motion Correction

C. Forman[1], M. Aksoy[2], M. Straka[2], J. Hornegger[1], and R. Bammer[2]
[1]Pattern Recognition Lab, Department of Computer Science, Friedrich-Alexander-University Erlangen-Nuremberg, Erlangen, Germany, [2]Department of Radiology, Stanford University, Stanford, CA, United States

INTRODUCTION – Patient motion during data acquisition is still a challenging problem for many MR sequences and can lead to considerable image artifacts. These often lower diagnostic confidence or even render images non-diagnostic. Recent publications have proposed methods to correct for brain motion by means of tracking the patient pose during the scan and try to adapt for possible changes in real-time [1,2,3]. Specifically, Aksoy *et al*. [3] presented an in-bore optical real-time motion-correction system that tracked a planar checkerboard marker with only one tiny spy camera mounted on the head coil. A drawback of this approach was that the marker had to be entirely within the field of view (FOV) of the camera. This in turn restricted the amount of motion that could be detected and subsequently corrected. To overcome this limitation, we propose a new marker design that is much more immune against the aforementioned limitations and show first *in-vivo* results.

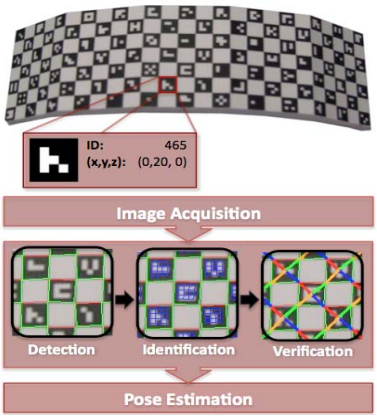

Figure 1 - The new marker design (top) and algorithm for detection and identification of squares is shown. First, the squares are detected, followed by the identification of the unique ID. Thereafter, the detected IDs are verified based on neighborhood information.

MATERIALS and METHODS – (a) System Description: The limited space inside the scanner bore entails that the camera is close to the patient's head. A common camera patient distance is between 5cm and 7cm. Thus, the restricted FOV of the camera affects the possible tracking range. To compensate this limitation we developed a new marker design based on the checkerboard pattern. In this marker, we encoded each square of the checkerboard by a unique and rotation invariant 9-bit code (Figure 1a). Each code identifies the location of the corresponding square with respect to the marker frame of reference. **(b) Pose Detection:** Within our tracking processor, the quads are detected on the camera image. The ID of each quad that is seen by the camera is then identified by binary classification. By means of a-priori knowledge about neighboring IDs on the marker one can verify the recognized IDs of all quads and improve fault-tolerance of erroneous quad detection. Lastly, the position of the marker – relative to the camera – can be estimated using the detected corners and their corresponding 3D object coordinates. As described in [2] the motion detected by the approach is then transformed into the scanner coordinate system and sent off to the sequencer via the Gigabit backbone of the MR scanner. Here, the sequencer adjusts gradients and RF frequencies – with minimum delay – at a maximum rate of ~30Hz to adapt the scan geometry to the detected patient pose. **(c) In-vivo Experiments:** For the *in-vivo* experiment, two sequences were used: **1)** axial and sagittal 3D SPGR sequence with TR/TE 9.5ms/4.1ms, flip angle=20°, slice thickness=1.5mm, FOV=24cm and a resolution of 192x192x96 **2)** T2-weighted spiral sequence with TR/TE=3000/90, 256x256 resolution, 32 interleaves. During the entire scan the volunteer was randomly moving his head simulating a patient suffering from Parkinson's disease. To adapt the scanner to these motion excursions, pose data from the new self-encoded marker were used. As a ground truth for optimal image quality, an additional scan was conducted where the patient was asked to maintain still.

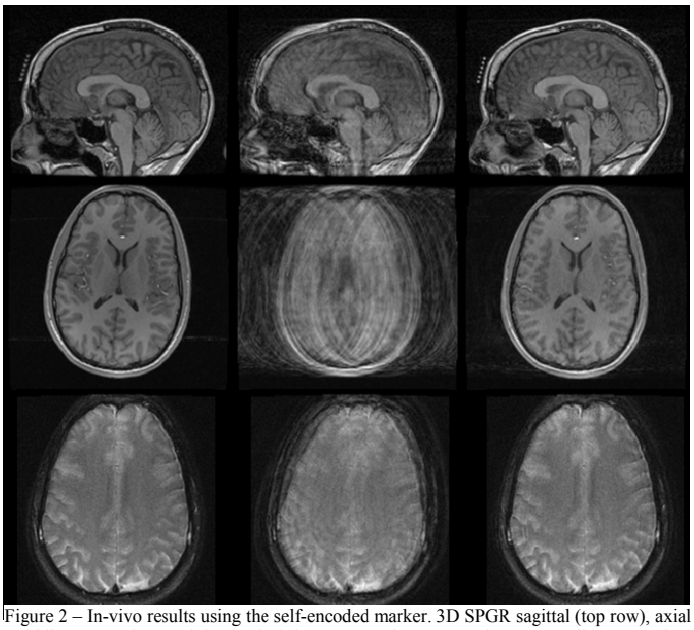

Figure 2 – In-vivo results using the self-encoded marker. 3D SPGR sagittal (top row), axial (middle row) and T2-weighted spiral (bottom row) images are shown. For all cases, patient motion causes significant artifacts on the data (middle column). These are removed by the optical tracking system (right column). Reference images are shown on the left column.

RESULTS – Figure 2 shows the resulting images for the *in-vivo* experiment using the 3D SPGR and the spiral sequences. The intensity and time pattern of motion excursion was comparable between both experiments. Without adaptive motion-correction, the resulting MRI images were severely degraded, whilst with adaptive motion-correction being active the images were of high quality and showed only marginal differences to the 'no motion' case. This is quite remarkable given the magnitude of motion used in these experiments. Of note here is also that the range of motion sustainable for correction was way larger than with the small checkerboard marker and essentially limited by the subject's head touching the coil.

DISCUSSION – In this study, we presented a new marker design for real-time prospective motion- correction. Recognizing the subpart of the marker, which was visible in the camera FOV, we were able to increase the range of motion that can be corrected. Thus, although huge motion occurred during the entire scan our software was still able to correct for it.

References [1] Zaitsev et al., NeuroImage, 31:1038-1050, 2006. [2] Aksoy et al, ISMRM, 2008 [3] Aksoy et al, ISMRM, 2009 **Acknowledgements** This work was supported in part by the NIH (1R01EB008706, 5R01EB002711, 1R01EB006526, 1R21EB006860, P41RR09784), Lucas Foundation, Oak Foundation, and GE Healthcare.